2010

Comparison of Secondary Islands in Collisional Reconnection to Hall Reconnection

L. S. Shepherd

P. A. Cassak

Comparison of Secondary Islands in Collisional Reconnection to Hall Reconnection

L. S. Shepherd and P. A. Cassak
Department of Physics, West Virginia University, Morgantown, West Virginia, 26506, USA
(Received 11 May 2010; published 2 July 2010)

Large-scale resistive Hall-magnetohydrodynamic simulations of the transition from Sweet-Parker (collisional) to Hall (collisionless) magnetic reconnection are presented; the first to separate secondary islands from collisionless effects. Three main results are described. There exists a regime with secondary islands but without collisionless effects, and the reconnection rate is faster than Sweet-Parker, but significantly slower than Hall reconnection. This implies that secondary islands do not cause the fastest reconnection rates. The onset of Hall reconnection ejects secondary islands from the vicinity of the X line, implying that energy is released more rapidly during Hall reconnection. Coronal applications are discussed.

DOI: 10.1103/PhysRevLett.105.015004 PACS numbers: 52.35.Vd, 52.30.Ex, 96.60.Iv, 96.60.qe

Magnetic reconnection is widely regarded as the mechanism underlying energy release in the solar corona during flares, coronal mass ejections, and coronal jets. The Sweet-Parker model [1,2] was the first self-consistent theory, but is far too slow to explain observations. Much has been invested in faster reconnection scenarios, such as collisionless (Hall) reconnection [3] in which the Hall term plays a key role [4,5] and seems fast enough to explain observed energy release rates [6]. Lately, the role of secondary islands (plasmoids) on Sweet-Parker reconnection has generated much interest. While they were discussed some time ago [7–9], systematic studies were not carried out until recently. It has been argued in various contexts that secondary islands make Sweet-Parker reconnection faster [7,10–12]. (Note, we are discussing secondary islands occurring during collisional reconnection, not those that occur after collisionless reconnection has begun [13].)

Secondary islands in Sweet-Parker reconnection may play a key role in coronal evolution. On the theoretical side, the reconnection rate places constraints on the dynamics. For example, if secondary islands make Sweet-Parker reconnection much faster or hasten the transition to fast reconnection, it cannot take place during preflare energy storage. If it remains slow, then it can occur while energy accumulates [14–16]. On the observational side, it was hypothesized that high density blobs in current sheets during solar eruptions are secondary islands [17,18]. Also, numerous observations of coronal reconnection processes display a slow phase preceding an eruptive event with an abrupt transition (e.g., [19–21]).

Secondary islands have been shown to appear spontaneously when the Lundquist number $S = 4\pi c_A L_{\rm SP}/\eta c^2$ exceeds $\sim 10^4$ [9], where $L_{\rm SP}$ is the half-length of the Sweet-Parker dissipation region, η is the resistivity, and c_A is the Alfvén speed based on the reconnecting magnetic field. Equivalently, this can be written as $\delta/L_{\rm SP} < 0.01$, where δ is the thickness of the dissipation region. A study of the linear phase of the instability [22] found a growth rate faster than the Alfvén transit time along the sheet. Recent simulations addressed the nonlinear reconnection rate E for high S, showing that it is considerably faster than the Sweet-Parker rate and its dependence on S becomes weak [23–25]. However, the simulations only go up to $S \sim 10^6$, so E is only 1 order of magnitude faster than the Sweet-Parker rate and it is not clear whether it will be fast or slow at larger S. Other relevant studies showed that E increases with the square root of the number of islands [24,26] and that secondary islands are suppressed when reconnection is embedded, meaning that the upstream field is smaller than the asymptotic field [27]. Many studies consider secondary islands caused by external random magnetic perturbations [28–31]. Other studies include the interaction of multiple islands [32] and a statistical model of multiple island interaction [33].

In addition to increasing the reconnection rate, secondary islands hasten the transition to Hall reconnection [26,34]. When a secondary island forms, the fragmented current sheet is shorter, so its Sweet-Parker thickness is smaller [24,26]. When the layer reaches ion gyroscales [35,36], Hall reconnection begins abruptly [14,26,37–39]. This was recently verified using collisional particle-in-cell (PIC) simulations [26,40].

The only previous studies to include both secondary islands and the Hall effect are Refs. [25,40], but numerical constraints forced S to be small enough that Hall reconnection began as soon as a secondary island formed. However, there should be a regime in which secondary islands are present without the Hall effect playing a role if the sheet is thicker than ion gyroscales. The goal of this study is to separate the two effects and ascertain which leads to dramatically larger reconnection rates.

In this Letter, the first simulations to separate the two effects are presented. There are three main results: (1) there is a regime in which secondary islands occur without collisionless effects entering; (2) the reconnection rate is faster than Sweet-Parker but significantly slower than Hall reconnection, which shows that secondary islands are not the cause of the highest reconnection rates; and (3) the onset of Hall reconnection ejects secondary islands in the vicinity of the X line. The latter two imply that the most efficient energy release occurs at Hall reconnection sites.

Numerical simulations are performed using the two-fluid code F3D [41]. Magnetic fields and densities are normalized to arbitrary values B_0 and n_0, velocities to the Alfvén speed $c_{A0} = B_0/(4\pi m_i n_0)^{1/2}$ where m_i is the ion mass, lengths to the ion inertial length $d_{i0} = c/\omega_{\rm pi}$, times to the ion cyclotron time $\Omega_{\rm ci}^{-1}$, electric fields to $E_0 = c_{A0}B_0/c$, and resistivities to $\eta_0 = 4\pi c_{A0} d_{i0}/c^2$.

The initial configuration is a double tearing mode with two Harris sheets, $B_x(y) = \tanh[(y + L_y/4)/w_0] - \tanh[(y - L_y/4)/w_0] - 1$, where w_0 is the initial current layer thickness and L_y is the system size in the inflow direction. Total pressure is balanced initially using a non-uniform density which asymptotes to 1. The temperature $T = 1$ is constant and uniform. A single X line is seeded using a coherent magnetic perturbation of amplitude 1.6×10^{-2} to rapidly achieve nonlinear reconnection. Initial random magnetic perturbations break symmetry so secondary islands are ejected. There is no initial out-of-plane (guide) magnetic field. Boundaries in both directions are periodic. Electron inertia is $m_e = m_i/25$. This value is acceptable since we focus on the onset of Hall reconnection at ion scales rather than electron scales.

Simulation parameters are chosen so reconnection will proceed in three distinct phases: Sweet-Parker without secondary islands, Sweet-Parker with secondary islands, and Hall reconnection. A very large system size $L_x \times L_y = 819.2 \times 409.6$ is employed with resistivity $\eta = 0.008$, corresponding to a global Lundquist number $S_g = L_x/\eta \sim 10^5$, which exceeds the Biskamp criterion of 10^4. To postpone secondary island onset, we choose $w_0 = 12.0$ which makes the reconnection embedded [27]. Embedding makes the Sweet-Parker layer thicker since $\delta \sim (\eta L_{\rm SP}/c_{\rm Aup})^{1/2}$, where $c_{\rm Aup}$ is the Alfvén speed based on the upstream magnetic field $B_{\rm up}$. For wide current layers, $B_{\rm up} \sim B_0 \delta/w_0$ [27], so eliminating $B_{\rm up}$ gives $\delta \sim (\eta L_{\rm SP} w_0)^{1/3} \sim 2.7$, where $L_{\rm SP} \sim L_x/4 \sim 200$ in our periodic system. Thus, the layer begins wider than d_i, and since $\delta/L_{\rm SP} > 0.01$, no secondary islands occur initially and the system undergoes Sweet-Parker reconnection. The inflow convects in stronger magnetic fields, so the current sheet self-consistently thins. Islands arise when $\delta/L_{\rm SP} \sim 0.01$, which gives $\delta \sim 2.0$. It has been shown [24,26] that if N X lines are present, δ decreases by a factor of $N^{1/2}$. For a single secondary island ($N = 2$), the layer shrinks to $\delta \sim 2.0/2^{1/2} \sim 1.4$. This exceeds d_i, so Sweet-Parker reconnection with secondary islands should persist. Hall reconnection only starts when $\delta \sim 1$, so three distinct phases occur.

A simulation is first performed with a grid scale $\Delta = 0.2$ and the results are qualitatively consistent with expectations. To assure Δ does not play a role, the simulations are redone with $\Delta = 0.1$, giving comparable results. Data is presented only from the high-resolution runs. The equations employ fourth-order diffusion with coefficient $D_4 = 1.75 \times 10^{-4}$ to damp noise at the grid scale. A smaller value of D_4 leads to a slightly larger Hall reconnection rate, but does not alter our key conclusions.

We now summarize the simulation results, followed by a careful justification of the conclusions. At early times, Sweet-Parker reconnection prevails. A secondary island first appears at $t \simeq 700$. Reconnection proceeds with the secondary island until $t \simeq 1780$, when Hall reconnection onsets. Thus, reconnection proceeds in three distinct phases including an extended phase with secondary islands but without the Hall effect triggered.

We compare the reconnection rate E in the three phases to each other and to theoretical predictions in Fig. 1(a), showing E vs time t as the solid (blue) line. We measure E as the time rate of change in the difference in magnetic flux function ψ between the main X line and O line. Dashed lines at $t = 700$ and 1780 denote where secondary islands and the Hall effect arise, respectively. Ignoring secondary islands, Sweet-Parker theory predicts $E \sim E_{\rm SP} \sim 0.006$, where $E_{\rm SP} \sim (\eta/L_{\rm SP})^{1/2}$. This assumes the magnetic field is its asymptotic value of 1. The measured value is $E \sim 0.004$, slightly lower than predicted as expected because $B_{\rm up} < 1$ (the reconnection is embedded). When N X lines are present, E scales as $E_{\rm SI} \sim E_{\rm SP}\sqrt{N}$ [26,27]. The measured rate of 0.005 is consistent with this for a single secondary island ($N = 2$). After the Hall effect onsets, E increases by an order of magnitude. Therefore, the reconnection rate with secondary islands is faster than Sweet-Parker, but significantly slower than Hall reconnection.

The transitions occur when predicted, as shown in Fig. 1(b). We plot δ, measured as the half-width at half-

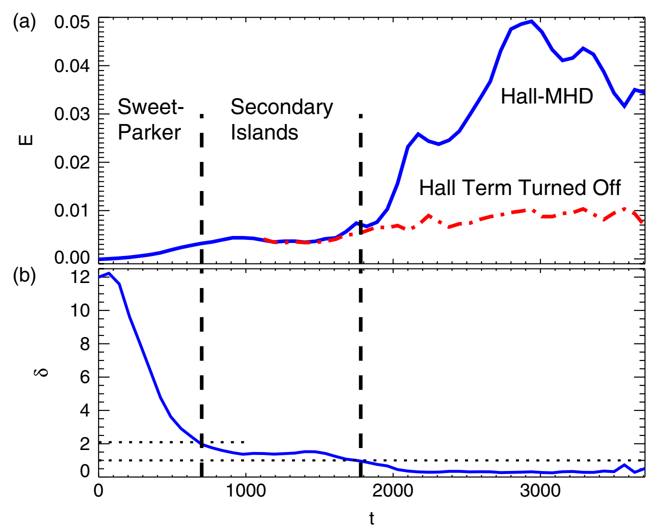

FIG. 1 (color online). (a) Reconnection rate E as a function of time t. The solid (blue) line is a two-fluid run. Dashed lines at $t \sim 700$ and 1780 indicate the onset of secondary islands and Hall reconnection, respectively. The dot-dashed (red) line shows E for a simulation restarted at $t = 1120$ with no Hall effect and $m_e = 0$. (b) Thickness δ of the dissipation region vs t. Horizontal dotted lines mark predicted δ for the onset of secondary islands ($\delta \sim 2$) and Hall reconnection ($\delta \sim 1$).

max of J_z in the inflow direction through the X line, vs t. The dotted lines at $\delta \sim 2$ and 1 show the predicted value when islands and the Hall effect should appear, respectively. These conditions are met at $t \simeq 700$ and 1780, in good agreement with the observed transitions.

The appearance of new physics can be seen in direct observations of the out-of-plane current density J_z. A two-dimensional time history plot of J_z in the outflow direction is plotted in Fig. 2. Only the half domain centered on the seeded X line is shown. The raw data is sampled at a rate of one frame per 70 time units, so linear interpolation is used to smooth data between time slices. The effect is cosmetic, not substantive. The color bar is stretched to enhance visibility of weaker currents. Early in time, J_z is structureless and extends the half-length of the domain, as expected during Sweet-Parker reconnection. A secondary island near $x = 0$ appears as a dark spot with associated strengthening of the fragmented current sheets. This occurs at $t \sim 700$, marked by the vertical dashed line. This agrees with Biskamp's criterion shown in Fig. 1(b). As time evolves, the island grows and δ shrinks. When $\delta \sim d_i$, Hall reconnection onsets and the current sheet becomes much shorter and intense, appearing as a sharp peak in J_z in Fig. 2. This begins at $t \sim 1780$, as also marked in Fig. 1(b).

There are two locations where Hall reconnection onsets. An X line near $x \simeq -70$ onsets slightly earlier than an X line at $x \simeq 70$. As Fig. 2 vividly shows, the latter X line is ejected from the dissipation region, along with the secondary island, which is ejected at the Alfvén speed. The ejection of the secondary island implies that the two effects do not (locally) coexist.

This current sheet has only a single secondary island and one may ask whether this result remains valid in more realistic settings with multiple islands. To address this, we show results from the other current sheet in our double tearing mode setup, which self-consistently develops multiple islands. Figure 3 shows J_z at 3 times near the onset of Hall reconnection. Panel (a) is just as Hall reconnection onsets at $x \simeq 20$, showing three existing secondary islands. The X line grows steadily, as shown in panel (b). Panel (c) shows that the single X line at $x \simeq 20$ is the only one to persist as all of the secondary islands are ejected. This suggests that the ejection of nearby secondary islands by Hall reconnection sites is a robust result, and may reasonably represent local behavior in a macroscopic current sheet.

We determine when the Hall effect begins to become important by using a time history plot of the out-of-plane Hall electric field $E_{\mathrm{Hz}} = J_y B_x / n$ in the inflow direction through the main X line, plotted in Fig. 4(a). The color bar is again stretched. The plot clearly shows that E_{Hz} does not contribute during the secondary island phase. A cut of E_{Hz} in time, taken at the solid (gray) line in Fig. 4(a), is plotted in Fig. 4(b). The onset time, defined as when E_{Hz} reaches 1% of its maximum value, is at $t \sim 1780$, the time that E begins to increase as seen in Fig. 1(a).

To emphasize differences between Sweet-Parker with secondary islands and Hall reconnection, we restart the

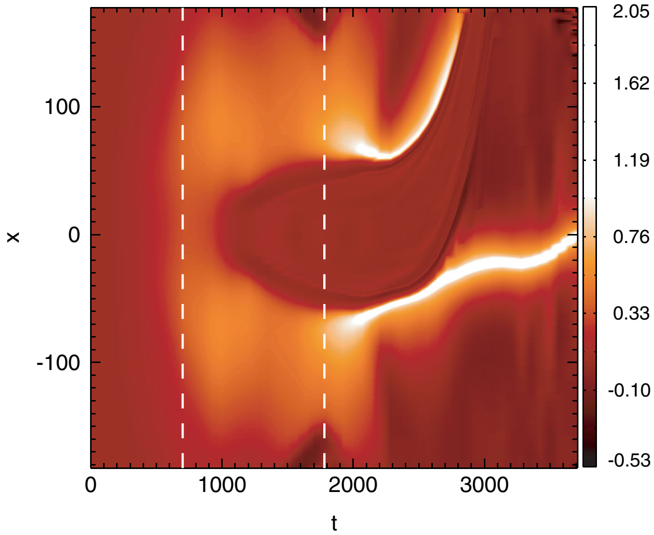

FIG. 2 (color). Time history plot of the out-of-plane current density J_z in the outflow direction. Dashed lines mark when a secondary island appears and when the Hall term onsets.

simulation at $t = 1120$ with the Hall effect and electron inertia disabled. The reconnection rate is plotted as the dot-dashed (red) line in Fig. 1(a). The value reaches $E \sim 0.009$ as the asymptotic upstream field reaches the dissipation region, in excellent agreement with the predicted value $E_{\mathrm{SI}} \sim E_{\mathrm{SP}}\sqrt{N} \sim 0.009$ with $N = 2$ for a single island. This rate is consistent with the largest scaling studies done to date [23]. Note, E remains nearly an order of magnitude slower than Hall reconnection. Although the present evidence is based on simulations only up to $S \sim 10^5$, it is clear that secondary island reconnection does not produce the fastest reconnection rates.

In summary, reconnection in marginally collisional plasmas can evolve in three distinct phases. In particular,

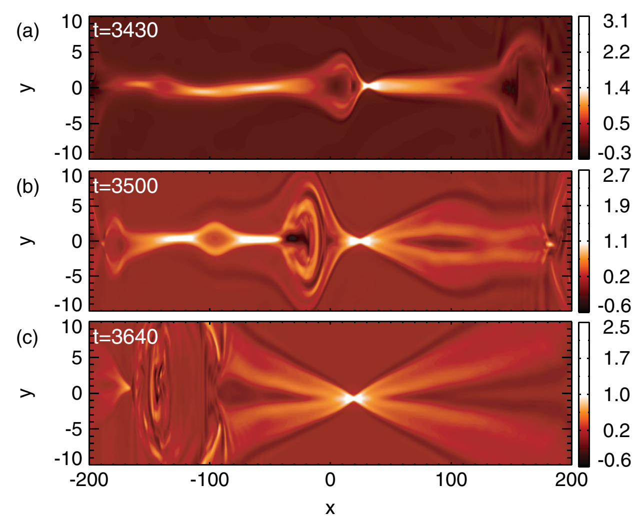

FIG. 3 (color). Time evolution of J_z from the other current sheet in our double tearing mode setup, showing the ejection of secondary islands when Hall reconnection onsets.

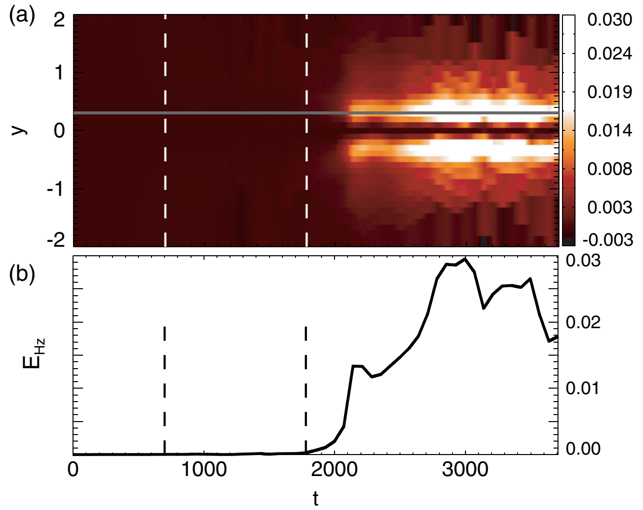

FIG. 4 (color). (a) Time history plot of the out-of-plane Hall electric field E_{Hz} in the inflow direction. (b) Plot of E_{Hz} vs t at the y location marked in panel (a).

Sweet-Parker reconnection with secondary islands can occur without triggering collisionless effects. The reconnection rate, though faster than classical Sweet-Parker, is an order of magnitude slower than Hall reconnection. The faster rate of Hall reconnection implies that secondary islands are ejected from the dissipation region at the Alfvén speed. The present simulations contain only a few secondary islands, but we expect that Hall reconnection sites locally eject previously existing islands in macroscopic current sheets. Thus, a majority of the magnetic energy is released at Hall reconnection sites.

The present results may be relevant two-phase reconnection events in the corona. In observations of flux emergence [19], a slow phase of reconnection preceded an abrupt transition to a fast phase ~30 times faster (compare the slopes in their Fig. 18). In observations of the contraction of magnetic loops in an impulsive flare [21], the contraction velocity abruptly increased by a factor of ~16. It is enticing to attribute these observations to an abrupt transition from resistive secondary island reconnection at a reconnection rate of $E \sim 0.01$ (consistent with implications of Refs. [23,26]) to Hall reconnection ~10 times faster as gyroscales are reached. The existing accuracy of both theory and observations make this identification premature, but it remains an exciting possibility.

Assumptions in this work that require further study include the omission of Ohmic heating, viscosity, Dreicer field effects, a guide field, three-dimensional effects, and using a Spitzer resistivity.

The authors gratefully acknowledge support by NSF Grant No. PHY-0902479, NASA's EPSCoR Research Infrastructure Development Program, and a WVU Faculty Senate Research Grant. This research used resources at National Energy Research Scientific Computing Center. We thank J. F. Drake for helpful conversations.

[1] P. A. Sweet, in *Electromagnetic Phenomena in Cosmical Physics*, edited by B. Lehnert (Cambridge University Press, Cambridge, England, 1958), p. 123.
[2] E. N. Parker, J. Geophys. Res. **62**, 509 (1957).
[3] J. Birn *et al.*, J. Geophys. Res. **106**, 3715 (2001).
[4] K. Malakit *et al.*, Geophys. Res. Lett. **36**, L07107 (2009).
[5] P. A. Cassak *et al.*, Phys. Plasmas 17, 062105 (2010).
[6] M. A. Shay *et al.*, Geophys. Res. Lett. **26**, 2163 (1999).
[7] W. H. Matthaeus and S. L. Lamkin, Phys. Fluids **28**, 303 (1985).
[8] W. H. Matthaeus and S. L. Lamkin, Phys. Fluids **29**, 2513 (1986).
[9] D. Biskamp, Phys. Fluids **29**, 1520 (1986).
[10] B. Kliem, in *Proc. CESRA Workshop*, edited by A. O. Benz and A. Krueger (Springer-Verlag, Berlin, 1995), Vol. 444, p. 93.
[11] A. Lazarian and E. Vishniac, Astrophys. J. **517**, 700 (1999).
[12] G. Lapenta, Phys. Rev. Lett. **100**, 235001 (2008).
[13] W. Daughton *et al.*, Phys. Plasmas **13**, 072101 (2006).
[14] P. A. Cassak, M. A. Shay, and J. F. Drake, Phys. Rev. Lett. **95**, 235002 (2005).
[15] D. A. Uzdensky, Astrophys. J. **671**, 2139 (2007).
[16] P. A. Cassak *et al.*, Astrophys. J. Lett. **676**, L69 (2008).
[17] A. Ciaravella and J. C. Raymond, Astrophys. J. **686**, 1372 (2008).
[18] J. Lin *et al.*, Astrophys. J. **693**, 1666 (2009).
[19] D. W. Longcope *et al.*, Astrophys. J. **630**, 596 (2005).
[20] R. Liu *et al.*, Astrophys. J. **696**, 121 (2009).
[21] R. Liu and H. M. Wang, Astrophys. J. Lett. **714**, L41 (2010).
[22] N. F. Loureiro *et al.*, Phys. Plasmas **14**, 100703 (2007).
[23] A. Bhattacharjee *et al.*, Phys. Plasmas **16**, 112102 (2009).
[24] P. A. Cassak *et al.*, Phys. Plasmas **16**, 102702 (2009).
[25] Y.-M. Huang and A. Bhattacharjee, Phys. Plasmas **17**, 062104 (2010).
[26] W. Daughton *et al.*, Phys. Rev. Lett. **103**, 065004 (2009).
[27] P. A. Cassak and J. F. Drake, Astrophys. J. Lett. **707**, L158 (2009).
[28] D. Smith *et al.*, Geophys. Res. Lett. **31**, L02805 (2004).
[29] G. Kowal *et al.*, Astrophys. J. **700**, 63 (2009).
[30] N. F. Loureiro *et al.*, Mon. Not. R. Astron. Soc. **399**, L146 (2009).
[31] M. Skender and G. Lapenta, Phys. Plasmas **17**, 022905 (2010).
[32] T. K. M. Nakamura *et al.*, Geophys. Res. Lett. **37**, L02103 (2010).
[33] R. L. Fermo *et al.*, Phys. Plasmas **17**, 010702 (2010).
[34] K. Shibata and S. Tanuma, Earth Planets Space **53**, 473 (2001).
[35] M. E. Mandt *et al.*, Geophys. Res. Lett. **21**, 73 (1994).
[36] Z. W. Ma and A. Bhattacharjee, Geophys. Res. Lett. **23**, 1673 (1996).
[37] A. Bhattacharjee, Annu. Rev. Astron. Astrophys. **42**, 365 (2004).
[38] P. A. Cassak *et al.*, Astrophys. J. **644**, L145 (2006).
[39] P. A. Cassak *et al.*, Phys. Rev. Lett. **98**, 215001 (2007).
[40] W. Daughton *et al.*, Phys. Plasmas **16**, 072117 (2009).
[41] M. A. Shay *et al.*, Phys. Plasmas **11**, 2199 (2004).